



## OPEN ACCESS

## EDITED BY

Jing Luo,  
Northwest Institute of Eco-  
Environment and Resources (CAS),  
China

## REVIEWED BY

Shufan Zhao,  
Ministry of Emergency Management,  
China  
Sudipta Sasmal,  
Indian Centre for Space Physics, India

## \*CORRESPONDENCE

Aleksandra Nina,  
sandrast@ipb.ac.rs

## SPECIALTY SECTION

This article was submitted to  
Atmosphere and Climate,  
a section of the journal  
Frontiers in Environmental Science

RECEIVED 28 July 2022

ACCEPTED 06 September 2022

PUBLISHED 29 September 2022

## CITATION

Nina A, Biagi PF, Pulinets S, Nico G,  
Mitrović ST, Čadež VM, Radovanović M,  
Urošev M and Popović LČ (2022),  
Variation in the VLF signal noise  
amplitude during the period of intense  
seismic activity in Central Italy from  
25 October to 3 November 2016.  
*Front. Environ. Sci.* 10:1005575.  
doi: 10.3389/fenvs.2022.1005575

## COPYRIGHT

© 2022 Nina, Biagi, Pulinets, Nico,  
Mitrović, Čadež, Radovanović, Urošev  
and Popović. This is an open-access  
article distributed under the terms of the  
[Creative Commons Attribution License  
\(CC BY\)](https://creativecommons.org/licenses/by/4.0/). The use, distribution or  
reproduction in other forums is  
permitted, provided the original  
author(s) and the copyright owner(s) are  
credited and that the original  
publication in this journal is cited, in  
accordance with accepted academic  
practice. No use, distribution or  
reproduction is permitted which does  
not comply with these terms.

# Variation in the VLF signal noise amplitude during the period of intense seismic activity in Central Italy from 25 October to 3 November 2016

Aleksandra Nina<sup>1\*</sup>, Pier Francesco Biagi<sup>2</sup>, Sergey Pulinets<sup>3</sup>,  
Giovanni Nico<sup>4</sup>, Srđan T. Mitrović<sup>5</sup>, Vladimir M. Čadež<sup>6</sup>,  
Milan Radovanović<sup>7,8</sup>, Marko Urošev<sup>7</sup> and Luka Č. Popović<sup>6,9,10</sup>

<sup>1</sup>Institute of Physics Belgrade, University of Belgrade, Belgrade, Serbia, <sup>2</sup>Physics Department, Università di Bari, Bari, Italy, <sup>3</sup>Space Research Institute, Russian Academy of Sciences, Moscow, Russia, <sup>4</sup>Istituto per le Applicazioni del Calcolo (IAC), Consiglio Nazionale delle Ricerche (CNR), Bari, Italy, <sup>5</sup>Novelic, Belgrade, Serbia, <sup>6</sup>Astronomical Observatory, Belgrade, Serbia, <sup>7</sup>Geographical Institute “Jovan Cvijić” SASA, Belgrade, Serbia, <sup>8</sup>South Ural State University, Institute of Sports, Tourism and Service, Chelyabinsk, Russia, <sup>9</sup>Department of Astronomy, Faculty of Mathematics, University of Belgrade, Belgrade, Serbia, <sup>10</sup>Faculty of Science, University of Banja Luka, Banja Luka, Bosnia and Herzegovina

Recent research shows reductions in the VLF signal noise amplitude that begin before particular earthquakes whose epicentres are more than 100 km away from the signal propagation path. In this paper, we extend this research to studying the noise amplitude during periods of intense seismic activity in a localized area. We analyse variations in the VLF signal noise amplitude over a period of 10 days (25 October–3 November 2016) when 981 earthquakes with the minimum magnitude of 2 occurred in Central Italy. Out of these events, 31 had the magnitude equal or greater than 4, while the strongest one had the magnitude of 6.5. We observe the VLF signal emitted by the ICV transmitter located in Sardinia (Italy) and recorded in Belgrade (Serbia). Bearing in mind that the trajectory of this signal crosses the area in which the observed earthquakes occurred, we extend the existing research to study of variations in the noise amplitude of the signal propagating at short distances from the epicentres of the considered earthquakes. In addition, we analyse the impact of a large number earthquakes on characteristics of the noise amplitude and its reductions before particular events. In order to examine the localization of the recorded changes, we additionally analysed the noise amplitude of two reference signals emitted in Germany and Norway. The obtained results show the existence of the noise amplitude reduction preceding individual strong or relatively strong earthquakes, and earthquakes followed by others that occurred in a shorter time interval. However, the additional noise amplitude reductions are either not pronounced or they do not exist before the considered events in periods of the reduced noise amplitude remain from previous earthquakes. Reductions in noise amplitudes for all observed signals indicate a larger perturbed area through which they spread or its closer location to the receiver. The analysis of daily values of parameters describing the noise amplitude reveals their variations start up to 2 weeks before the seismically active period occurs.

## KEYWORDS

earthquakes, earthquake precursor, VLF signal, noise amplitude, ionosphere, intense seismic activity

## 1 Introduction

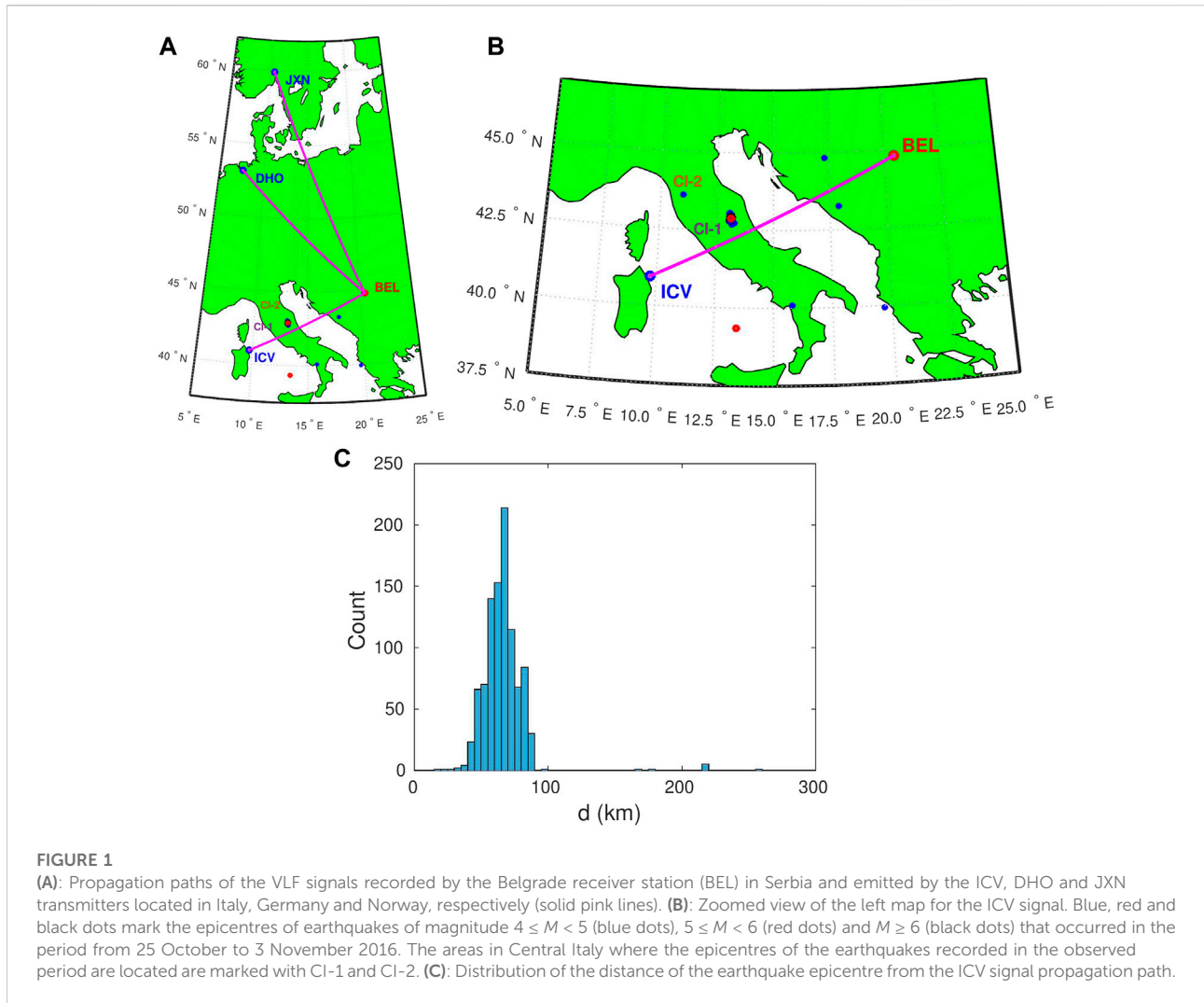
In a large number of scientific studies published in this and the previous century, different types of ionospheric disturbances that precede earthquakes (EQs) are shown (Davies and Baker, 1965; Leonard et al., 1965; Yuen et al., 1969; Calais and Minster, 1998; Maekawa et al., 2006; Sasmal and Chakrabarti, 2009; Chakrabarti et al., 2010; Oyama et al., 2016; Xiong et al., 2021; He et al., 2022; Molina et al., 2022). The repetition of the same or very similar characteristics of these disturbances indicates the possibility that they are precursors of earthquakes, which is why a relevant both theoretical and experimental research is of great importance. In the first case, studies provide several theoretical explanations for the relationship between ionospheric disturbances and lithospheric processes associated with earthquakes, and they are based on thermal and chemical mechanisms as well as on generation of acoustic and electromagnetic waves, and quasi constant local electric field (Sorokin and Yashchenko, 1999; Pulinets and Boyarchuk, 2004; Liperovsky et al., 2008; Korepanov et al., 2009; Pulinets and Ouzounov, 2011; Fu et al., 2015). On the other hand, the observations are based on remote sensing of the high (using ionosonde/digisonde and radar) and lower (using very low/low frequency (VLF/LF) radio signals) ionosphere as well as integral information about the entire ionosphere obtained by the Global Navigation Satellite System (GNSS) signals (Biagi et al., 2001b, 2011; Hegai et al., 2006; Perrone et al., 2018). In addition, measurements by satellites orbiting in the ionosphere (e.g., Detection of Electro-Magnetic Emissions Transmitted from Earthquake Regions (DEMETER) satellite) are used for relevant studies (Němec et al., 2009).

Previous studies indicate that typical perturbations (variations of the electron density (positive and negative) at specific altitudes of the ionosphere registered by ionosondes, the total electron content (TEC) variations registered by GNSS receivers, changes in the VLF/LF signal amplitude (or phase), its periodic fluctuations and the “terminator time” shift) are registered in all ionospheric regions mostly a few days before the occurrence of stronger earthquakes (Hayakawa, 1996; Molchanov et al., 1998; Biagi et al., 2001b, 2006; Miyaki et al., 2001; Molchanov et al., 2001; Pulinets and Boyarchuk, 2004; Rozhnoi et al., 2004; Yamauchi et al., 2007; Hayakawa et al., 2010; Liu et al., 2018; Perrone et al., 2018; Pulinets et al., 2022). However, recent research presented in Nina et al. (2020) and Nina et al. (2021a) points out a possibility for a new type of precursor that occurs up to a few tens of minutes before an EQ (including some cases of weak earthquakes whose magnitude can be less than 3) and manifests itself through a reduction in the VLF

signal amplitude and phase noise, respectively. These studies present analyses of several EQs whose epicentres were relatively close to the considered signal propagation path. In these analysed cases, the detected individual reductions can be clearly associated with individual EQs. In other words, the disturbance in the environment in which the signal propagates either ends quickly enough and do not affect disturbances that could potentially be associated with further EQs or is further amplified before an another event. A possible explanation for this may be the fact that the analysed earthquakes occurred in several remote locations (Serbia, Italy, Tyrrhenian Sea and Western Mediterranean Sea). However, the question arises as to how a large number of EQ events whose epicentres are located in close locations and that occur in a relatively short time period affect the signal noise properties. The importance of this issue can be seen in the fact that in the DHO and GQD signals with a small noise amplitude during the time periods observed in the study Nina et al. (2020) no reduction of the noise amplitude was recorded, which, consequently, requires the examination of the existence of an additional reduction of this parameter if it is already significantly reduced by some previous EQ. The analysis of this issue is the main aim of this paper. In addition, the aims of this research are to explore the VLF signal prior the considered EQs in order to confirm our finding of the noise amplitude reduction in the case of EQs that occurred during the period when the noise amplitude corresponds to that in quiet conditions and, for the first time, to explore the daily characteristics of the VLF signal noise amplitude in time periods before, during and after the considered intensive seismic activity.

In this study, we analyse the time evolution of the noise amplitude of the ICV signal transmitted in Italy and recorded in Serbia in the period from 25 October to 3 November 2016 which was the time period of intense seismic activity (PISA). During this period there were 981 earthquakes in Central Italy of minimum magnitude 2, out of which there were 31 cases with magnitudes equal or greater than 4. In addition, we analyse daily characteristics of the noise amplitude in the time period from 1 October to 22 December in order to examine long-term variations around intense seismic activity located at a small area. To study localization of the perturbed atmospheric part, we analyse two additional VLF signals emitted by the DHO (Germany) and JXN (Norway) transmitters and received in Belgrade, Serbia.

The paper is organised as follows. The descriptions of observations, considered events, and the applied procedures for data processing are presented in Section 2. Section 3 shows the obtained results and their discussion. Finally, the conclusions of this study and the list of the opened questions are given in Section 4.



## 2 Observations and data processing

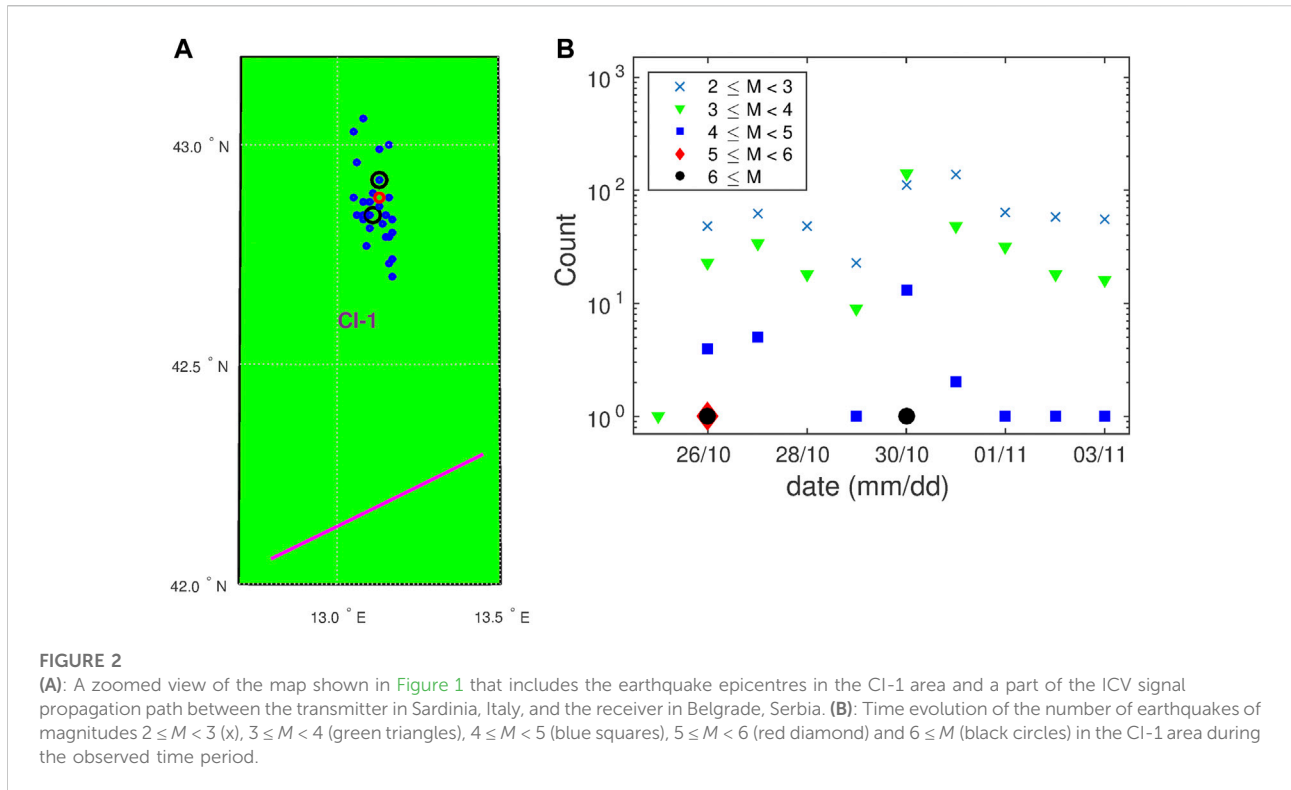
### 2.1 Observational setup and study area

The study presented in this paper is based on the processing of the VLF signal amplitudes recorded by the Absolute Phase and Amplitude Logger (AbsPAL) receiver in Belgrade, Serbia (44.8 N, 20.4 E). The data recorded by this receiver are used in many analyses (Žigman et al., 2007; Grubor et al., 2008; Kolarski et al., 2011). Here, we analyse three signals emitted by the ICV, DHO and JXN transmitters located in Isola di Tavolara, Sardinia, Italy (40.92 N, 9.73 E), Rhauderfehn, Germany (53.10 N, 7.60 E) and Kolsas, Norway (59.91 N, 10.52 E), respectively. Their propagation paths are shown in Figure 1A.

The focus of this research is on the ICV signal amplitude processing because, as the map shows, its propagation path to Belgrade is closest to the epicentres of the observed set of earthquakes marked as blue, red and black points depending

of their magnitudes (a zoomed map view of the signal propagation area is given in the upper right panel). In addition, a study given in Nina et al. (2020) indicates the appropriate noise amplitude reductions for this signal, and, consequently, shows that it is suitable for relevant analyses. This is important because the influence of the signal characteristics on the possibility of detecting the considered specified form of amplitude change has not been investigated yet, and by choosing this signal we eliminate the possibility of no detection of the observed change due to e.g. insufficient sensitivity of the selected signal to atmospheric noise variations.

We analyse the signals emitted by the DHO and JXN transmitters in order to examine the influence of the receiver, and electronic and electrical devices close to it on the signal noise amplitude, and the localization of the detected changes. Here, we point out that variations in the signal emission relevant for the study are eliminated by analysing its amplitude recorded by the receiver located in Kilpisjärvi, Norway (see Section 2.3).



## 2.2 Analysed events

In the detailed analysis of the ICV signal amplitude, we observe the time period from 25 October to 3 November 2016 when seismic activity in Central Italy was very intense. In Figure 1, we show a map of the area where the observed signal propagates, and the epicenters of EQs that occurred during the analysed time period, out of which 981 (with the magnitude,  $M$ , equal or greater than 2) occurred in Central Italy. For clarity, we show the epicenters of earthquakes of minimum magnitudes 3.9 (blue dots), 5 (red circle) and 6 (black circles) on this map. As can be seen in the map, these epicenters are grouped into two localized areas marked as CI-1 and CI-2 (the maximum earthquake magnitude in this area is 3.9, so we included this value in the epicentre display in the map). The histogram of the distances  $d$  between the epicenters of all considered EQs and the signal propagation path is shown in Figure 1C where one can see that  $d$  is smaller than 100 km in almost all (more than 99%) cases. The number of the EQ events with  $40 \text{ km} < d < 90 \text{ km}$  is 963 which is 98.2% of the total number of observed EQs. The distance  $d$  is bigger than 100 km in only 8 cases and corresponds to the events that took place at the CI-2 area.

Considering that the epicenters of EQs that occurred in the CI-2 area are significantly further from the signal propagation path ( $d$  is between 168 and 259 km) than those occurred in the CI-1 area ( $d$  is below 100 km), and that their magnitudes are below 4, we focus on events in the CI-1 area. A zoomed view of the map for this area

with 31 EQ epicentre locations (for  $M \geq 4$ ) and part of the observed signal path are given in the left panel, while the numbers of EQ events per day with magnitudes between 2 and 3, 3 and 4, 4 and 5, 5 and 6, and greater than 6 are shown in Figure 2B. The list of analysed 31 earthquakes (magnitudes of 4) with their characteristics (times of their events, epicentre locations, depths, magnitude values and types, and epicentre distances from the ICV signal propagation path) is given in Table 1.

As one can see in the map shown in Figure 1, the upper right panel, two additional EQs also occurred relatively close to the considered signal propagation path (in Bosnia and Herzegovina). Their magnitudes are 4.2 (31 October 2016, 09:38:13 UT, (43.26N,17.88E)) and 3.9 (3 November 2016, 15:04:03 UT, (44.82N,17.3E)). In the first case, no reduction of  $A_{\text{noise}}$  is recorded, while in the period around the second event the ICV signal is not recorded in Belgrade. In the observed period, there were additional two EQs of magnitudes of 2.6 and 2.5 in Bosnia and Herzegovina, and Serbia, respectively. In the first case, the analysed reduction is not recorded, while, in the second case, the time of EQ is in the period of occurrences of two EQs of higher magnitudes (4.6 and 3.9) in the CI-1 area which are much more likely to be associated with the corresponding detected  $A_{\text{noise}}$  reduction. The strongest EQ outside Central Italy of magnitude 5.8 occurred in the Tyrrhenian Sea (28 October, 20:02:49 UT, (39.35N,13.44E)). As will be seen in Section 3,  $A_{\text{noise}}$  is low throughout the day and although its slight reduction in the period around this EQ is visible, it is not possible to reliably link these two phenomena.

**TABLE 1** List of the main studied earthquakes. Data for EQ date, time  $t$ , epicentre locations (latitude (LAT) and longitude (LON)) and magnitudes (M) are given in <http://www.emsc-csem.org/Earthquake/>. Distances between the EQ epicentres and signal propagation path are indicated as  $d$ .

No	Date	Time UTC	Latitude	Longitude	Depth	Magnitude Type	Magnitude	Distance
1	2016/11/03	00:35:01	43.03	13.05	8	Mw	4.8	85.0
2	2016/11/02	19:37:52	42.89	13.11	10	ML	4	68.9
3	2016/11/01	07:56:39	43	13.16	10	Mw	4.9	78.0
4	2016/10/31	07:05:45	42.83	13.17	20	Mw	4.2	60.7
5	2016/10/31	03:27:40	42.77	13.09	11	mb	4.3	57.7
6	2016/10/30	18:21:09	42.79	13.15	10	ML	4.2	57.5
7	2016/10/30	13:34:54	42.8	13.17	9	ML	4.6	57.8
8	2016/10/30	12:07:00	42.84	13.08	10	ML	4.6	65.1
9	2016/10/30	11:58:17	42.84	13.06	10	ML	4	65.8
10	2016/10/30	11:21:09	43.06	13.08	2	ML	4.1	86.9
11	2016/10/30	10:19:26	42.82	13.14	11	ML	4.1	60.9
12	2016/10/30	08:35:58	42.83	13.08	10	mb	4.6	64.1
13	2016/10/30	07:34:47	42.92	13.13	10	ML	4	71.1
14	2016/10/30	07:13:06	42.73	13.16	10	mb	4.5	51.2
15	2016/10/30	07:07:54	42.7	13.17	2	ML	4.2	47.9
16	2016/10/30	07:05:56	42.79	13.16	8	ML	4.1	57.1
17	2016/10/30	07:00:40	42.88	13.05	10	ML	4.1	70.1
18	2016/10/30	06:55:40	42.74	13.17	13	ML	4.1	51.8
19	2016/10/30	06:40:18	42.84	13.11	10	Mw	6.5	63.9
20	2016/10/29	16:24:33	42.81	13.1	11	mb	4.4	61.3
21	2016/10/27	17:22:23	42.84	13.1	9	ML	4.2	64.3
22	2016/10/27	08:21:46	42.87	13.1	9	Mw	4.4	67.3
23	2016/10/27	03:50:24	42.99	13.13	9	Mw	4.2	78.1
24	2016/10/27	03:19:27	42.84	13.15	9	mb	4.4	62.5
25	2016/10/27	00:21:32	42.96	13.06	10	mb	4.2	77.7
26	2016/10/26	23:52:32	42.82	13.14	10	mb	4	60.9
27	2016/10/26	21:42:02	42.86	13.13	10	Mw	4.7	65.2
28	2016/10/26	21:24:51	42.87	13.08	9	mb	4.1	68.0
29	2016/10/26	19:18:07	42.92	13.13	8	Mw	6.1	71.1
30	2016/10/26	19:16:57	42.88	13.16	8	ML	4.3	66.1
31	2016/10/26	17:10:36	42.88	13.13	9	Mw	5.5	67.2

Based on the previous analysis, it can be concluded that the noise amplitude reductions can be related to the EQs that occurred in the CI-1 area and that other EQ events do not significantly affect the presented analysis.

In addition to the detailed analysis of the ICV signal amplitude for the indicated 10 days, we analysed the period from 1 October to 22 December to examine long-term variations around the seismological active period.

## 2.3 Analysis of other potential influences on the signal amplitude

As stated in the literature (Biagi et al., 2011; Nina et al., 2020), there are numerous causes of variations in signal characteristics.

They refer both to natural sources of disturbances and to technical changes in the emission and reception of signals due to, for example, electric or electronic devices operating nearby the receiver, electric cables without good shielding, amateur radios operating in the zone, an improperly grounded receiver, or natural electromagnetic emissions from nearby faults or micro-fractured zones. For this reason, it is necessary to check the presence of influence of these factors on the signal characteristics important for this study.

- Natural conditions. The main potential natural causes of changes in a VLF signal propagation are related to meteorological and geomagnetic conditions, and variations in radiation from the Sun and other sources in the Universe.

- Meteorological conditions can cause disturbances in signal characteristics of different durations. However, typical signal variations caused by lightning (see, for example, Wang et al. (2020) and references therein) do not have the same characteristics as those analysed in Nina et al. (2020) as a potential EQ precursor. In addition, there were no significant meteorological events in the area near the ICV signal route from Sardinia to Belgrade in the observed period according to the European Severe Weather Database (<https://eswd.eu/cgi-bin/eswd.cgi>). The only recorded north wind was on 2 November 2016.
- Geomagnetic conditions. The values of the Kp index were below 5 during this time, except in seven and three three-hour periods when they were  $\geq 5$  and  $\geq 6$ , respectively ((Matzka et al., 2021), [https://www-app3.gfz-potsdam.de/kp\\_index/Kp\\_ap\\_Ap\\_SN\\_F107\\_since\\_1932.txt](https://www-app3.gfz-potsdam.de/kp_index/Kp_ap_Ap_SN_F107_since_1932.txt)). Although the values of 5 and 6 in the NOAA scale are indicators of minor and moderate geomagnetic storms, respectively (<https://www.swpc.noaa.gov/noaa-scales-explanation>), the comparison of these periods with the time evolution of the noise amplitude show the indicated storms cannot be related to variations in the intensity of this parameter.
- Extraterrestrial electromagnetic radiation. Changes in the D-region electron density (the plasma parameter that is significant for a VLF signal propagation) are dominantly influenced by the solar hydrogen Ly $\alpha$  line in quiet conditions (Mitra, 1974; Nina et al., 2021b) and the soft X-radiation produced during solar X-ray flares (Thomson et al., 2005; Kolarski et al., 2011; Basak and Chakrabarti, 2013; Schmitter, 2013; Ammar and Ghalila, 2016; Chakraborty and Basak, 2020). In both cases, these impacts are significant during the daytime period. Based on the obtained noise amplitude values in Nina et al. (2020), it can be concluded that the noise amplitude of the observed signal is not affected by the daily variations of the mentioned Ly $\alpha$  radiation. In addition, during the observed period, no solar X-ray flares of class C and stronger, which can affect VLF signal characteristics, were recorded ([https://hesperia.gsfc.nasa.gov/goes/goes\\_event\\_listings/](https://hesperia.gsfc.nasa.gov/goes/goes_event_listings/)). Based on this, we can conclude that solar radiation cannot be the cause of the significant variations in the noise amplitude analysed in this study.

The changes in the signal that are indicated as the detection of gamma ray burst in Inan et al. (2007) are not recorded, while those shown in Nina et al. (2015) do not correspond to the changes analysed in this study.

- Non-natural conditions. Amplitude variations that result in reductions of its noise amplitude can also be consequences of variations in the signal emission and/or reception. In

order to eliminate the presence of these influences, we analyse the amplitude of the ICV signal recorded by the Kilpisjärvi ULTRA Data receiver (to check variations in the emission of the observed ICV signal) and the DHO and JXN signals emitted in Germany and Norway, respectively, and received by the AbsPAL receiver in Belgrade (to check variations in the reception of the signal by the used receiver). Comparisons with the analysed ICV signal noise amplitude recorded in Belgrade show the following:

- Signal emission. In contrast to the noise amplitude of the ICV signal recorded in Belgrade, which does not have typical daily variations, the noise amplitude of this signal recorded in Kilpisjärva is greater during daytime than during nighttime conditions. Ignoring these periodic changes, the obtained values do not show noise amplitude reductions that match those visible in the data recorded in Belgrade. This suggests that the analysed reduction does not occur in the signal emission.
- Signal reception. In addition to the influence of changes in the signal emission, variations in its reception can occur due to changing characteristics of the environment in which it spreads, and technical problems (including the influence of additional electric and electronic devices near the receiver) during its reception. Bearing in mind that this is one of the pioneer studies and that we cannot *a priori* assume the borders of the area of potential influence of seismic changes on the atmosphere, we compare the noise amplitude of the ICV signal with the corresponding values related to two additional signals recorded by the same receiver in Belgrade. A detailed analysis of this comparison, given in Section 3.1.2, shows that the noise amplitudes reductions recorded for ICV signal also occur for other signals (in all cases for EQs of magnitude over 5, and for the DHO signal for EQs of magnitude below 5 (during October 27)). However, the intensities of these reductions are different, and their relationships cannot be established either with the intensity of the signal amplitudes or with the noise amplitudes corresponding to quiet conditions. For this reason, we can conclude that these reductions are most likely due to changes in the atmosphere, i.e. they do not result from technical problems in reception.

Based on the previously presented checks, we are now able to present the following analysis of the potential relationship of the recorded noise amplitude reductions with the considered EQs.

## 2.4 Data processing

The procedure for the determination of the noise amplitude,  $A_{\text{noise}}$ , used in this study is described in Nina et al. (2015) and applied in the studies of the noise reductions in the amplitude

and phase presented in Nina et al. (2020) and Nina et al. (2021a), respectively. It is based on processing of the signal amplitude  $A$  recorded by the AbsPAL receiver with time resolution of 0.1 s, and on determining of:

- The basic amplitude  $A_{\text{base}}(t)$  at the time  $t$  as the mean value of the amplitude values in the time bin  $(t - \Delta t, t + \Delta t)$ :

$$A_{\text{base}}(t) = \frac{1}{i_{t+\Delta t} - i_{t-\Delta t} + 1} \sum_{i=i_{t-\Delta t}}^{i=i_{t+\Delta t}} A(i) \quad (1)$$

where  $i_t$  is the ordinal number of the element in the array of the recorded amplitude values corresponding to the time  $t$ .

- The deviation of the signal amplitude  $A(t)$  from the basic amplitude  $A_{\text{base}}$  at the time  $t$  using expression:

$$dA(t) = |A(t) - A_{\text{base}}(t)|. \quad (2)$$

- The noise amplitude  $A_{\text{noise}}$  in the defined time bins as the maximum of the array  $B$  obtained by reducing the array  $|dA|$  of  $N$  values to the array of  $N^*$  values by eliminating  $p$  percent of the highest values ( $B(1 : N^*) = \text{sort}(|dA|)(1 : N^*)$ ):

$$A_{\text{noise}} = \max(B). \quad (3)$$

As in the study presented in Nina et al. (2020) and Nina et al. (2021a), in this analysis we assumed that  $p = 5\%$  (the study given in Nina et al. (2015) indicates that the choice of this value has no essential significance for relevant analyses).

In this study, the examination of variations in daily noise amplitude characteristics is based on the analysis of its minimum, maximum, mean and median values, as well as the standard deviation from 0 to 24 h for the period from 1 October to 22 December.

### 3 Results and discussions

In this study, we investigate the existence of the VLF signal noise amplitude reductions lasting from several tens of minutes to several hours during the time periods around earthquakes (described in Nina et al. (2020)). Bearing in mind that almost 1000 EQs (31 of them had magnitudes 4 or greater) were registered in Central Italy in just 10 days, we also analyse the presence of long-term variations in the noise amplitude. Therefore, the obtained results and their analysis are presented in two parts related to the noise amplitude time evolution (Section 3.1) and daily characteristics of the noise amplitude (Section 3.2).

#### 3.1 Time evolution of the noise amplitude

During the period from 26 October to 3 November, 31 earthquakes with the minimum magnitude of 4 were registered in the CI-1 area. In this Section we study

characteristics of the ICV signal amplitude (Section 3.1.1) and compare the obtained amplitude noise reduction with those corresponding to two referent signals (Section 3.1.2) in order to examine localization of the considered changes.

##### 3.1.1 Time evolution of the ICV signal noise amplitude

In Figure 3, we show time evolutions of the recorded ICV signal amplitude,  $A$ , its deviation from the corresponding basic curve,  $dA$ , and the noise amplitude,  $A_{\text{noise}}$ , for this period and for 1 day that precedes it in order to show the analysed parameters during relatively quiet conditions. The vertical lines in the lower panels indicate the time of the considered EQ occurrences and the horizontal ones (given for a better overview of the  $A_{\text{noise}}$  reductions and their easier comparison during the observed time interval) represent the noise amplitude values of 1.5 and 1 dB (they are determined as values which are about 0.5 and 1 dB lower than the ICV signals noise amplitude in the “quiet” time period before PISA which is about 2 dB). In these panels one can notice: (1) the absence of mid-term (of several tens of minutes and longer) periodic daily variations of  $A_{\text{noise}}$  (that is in agreement with the analysis given in Nina et al. (2020)), (2) short-term increases of this parameter during the solar terminator periods (ignored in the further analysis relevant to the potential connection of the considered signal characteristics and earthquakes), and (3) three profiles of the noise amplitude reduction behaviour (seen in Figure 4):

- (1) Type I (left panel)—the amplitude noise reduction is a consequence of both the increasing lower and decreasing higher amplitude values. In this case, the tendency of the  $A_{\text{base}}$  time evolution does not change. This type is also recorded in the case of Kraljevo EQ (Nina et al., 2020).
- (2) Type II (middle panel)—the amplitude noise reduction is a consequence of increasing lower amplitude values. In this case, the highest amplitude values do not decrease, which affects the increase of the basic amplitude values.
- (3) Type III (right panel)—the amplitude noise reduction is a consequence of decreasing the upper amplitude values to previously minimum values or even lower. In this case, the lower amplitude values do not increase and the basic amplitude decreases.

The analysis of the presented parameters shows the following:

- 25 October. During this day, no strong EQs were recorded in the CI-1 area. A several-hour  $A_{\text{noise}}$  reduction that is visible in the afternoon corresponds to the time period around EQ of magnitude 3.9 in the CI-2 area. In other periods, the approximate value of  $A_{\text{noise}}$  is 2 dB, and it can be considered as  $A_{\text{noise}}$  in quiet conditions.

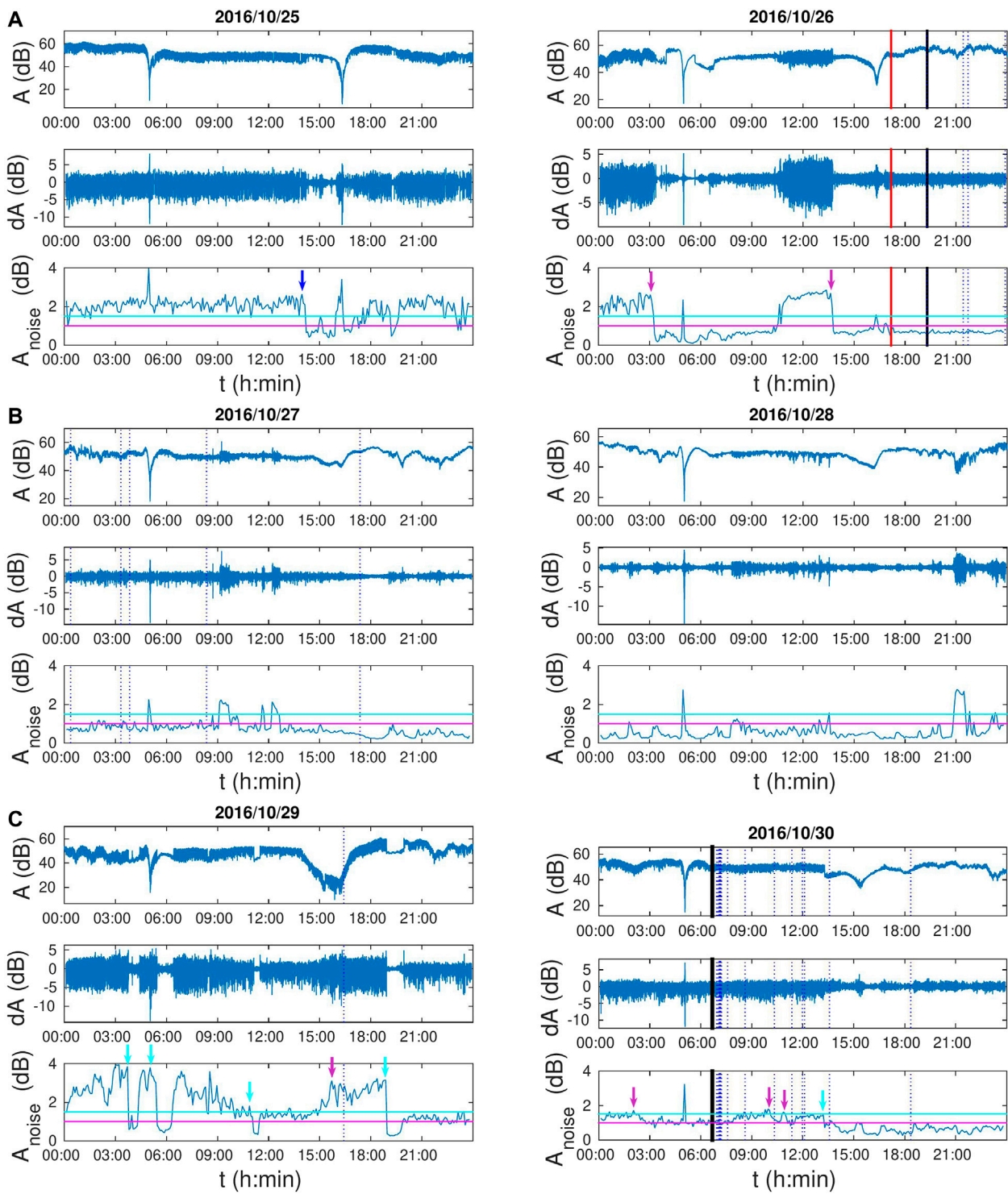
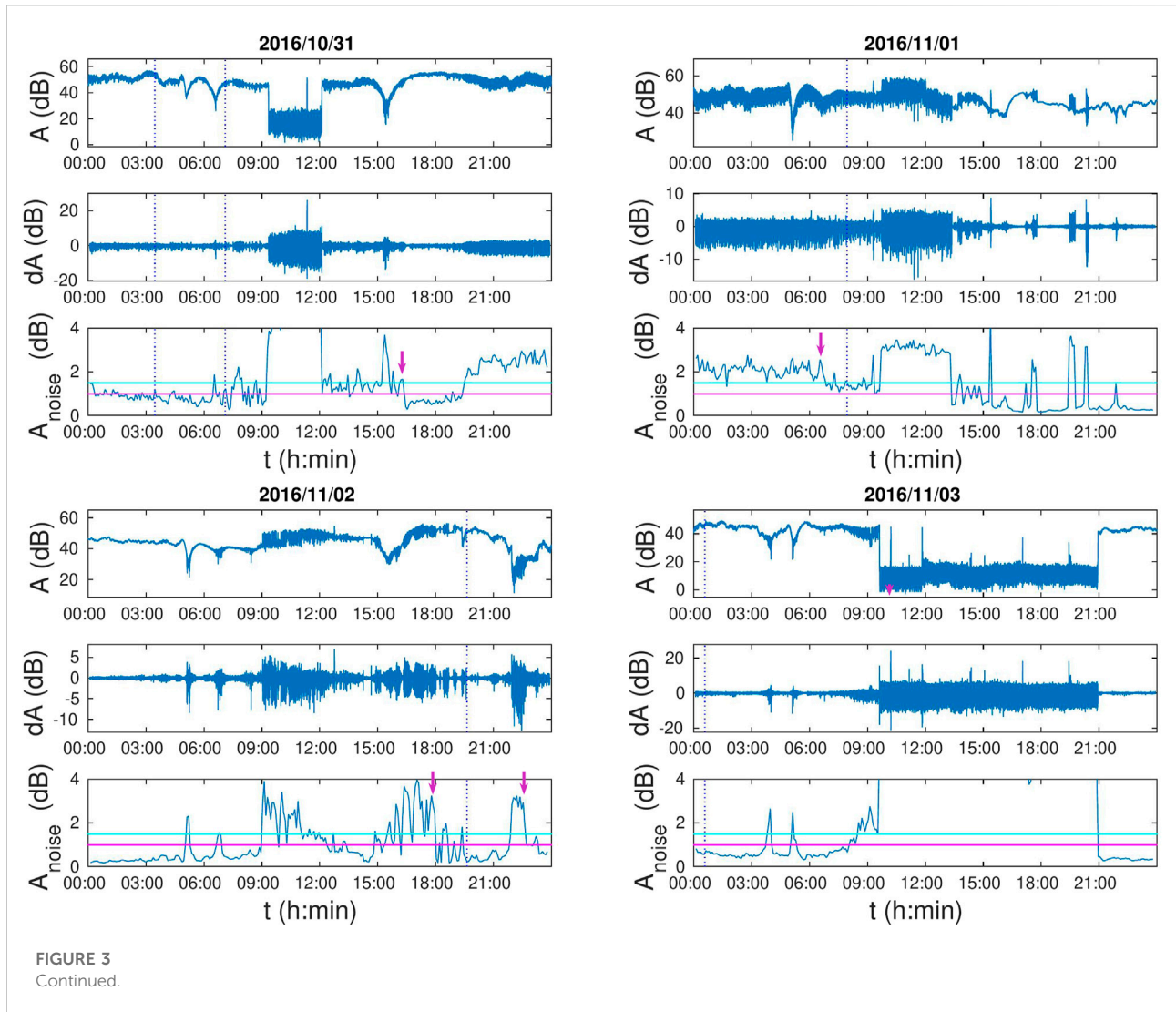


**FIGURE 3**

The time evolutions of the recorded amplitude  $A$  (A), its deviation,  $dA$ , from the base curve (B), and the noise amplitude,  $A_{noise}$ , (C) for the period of 25 October to 3 November 2016. Vertical lines indicate the times of earthquakes of magnitude  $4 \leq M < 5$  (blue dot lines),  $5 \leq M < 6$  (red line) and  $6 \leq M$  (black lines). Horizontal magenta and cyan lines indicate the amplitude of 1 and 1.5 dB, respectively. The beginnings of the amplitude noise reductions of Type I, II and III are indicated by the magenta, blue and cyan arrows, respectively.





- 26–28 October. The expected values of  $A_{\text{noise}}$  under quiet conditions are visible at the beginning of 26 October. Its reduction to values below 1 dB begins a little after 3 UT, which is about 14 h before the first considered large EQ of magnitude 5.5. This reduction is followed by an increase of  $A_{\text{noise}}$  to values between 2 and 3 dB in a period of about 3 h starting at about 10:40 UT. After that,  $A_{\text{noise}}$  drops again back to values below 1 dB (at approximately 13:40 UT). This second reduction starts about 3.5 h before the mentioned EQ at 17:10 UT. Both of these  $A_{\text{noise}}$  reductions are of Type I. However, in the case of the first one, no earthquakes were recorded near the considered signal propagation path, which open the question: Can more reduction of  $A_{\text{noise}}$  occur before a strong earthquake or more (relatively) strong earthquakes (in this case, EQs of magnitudes of 5.5 and 6.1 and 7 EQs of magnitudes of 4–4.7 in a period shorter than 11 h)? The values of  $A_{\text{noise}}$  continued to be low for the next 2 days. In that

period, 5 EQs (of magnitudes of 4.2 (three events) and of 4.4 (two events)) were recorded on October 27, while there were no earthquakes of magnitude greater than 4 on October 28. It is important to note here that there were no additional significant reductions that could be linked with the mentioned five EQs.

- 29–31 October.  $A_{\text{noise}}$  exceeds 2 dB at the beginning of 29 October and it is very unstable until about 20 UT. During that period, four reductions of  $A_{\text{noise}}$  below 1.5 dB (Type 3) that cannot be associated with EQs (not even those of magnitude less than 4) and one of Type 1 preceding EQ of magnitude 4.4 are visible. During the period of this reduction, a large number of less intense EQs were recorded. After 20 UT,  $A_{\text{noise}}$  is stabilized between 1.5 and 2 dB until around 14 UT on 30 October. During this time period, an EQ of magnitude 6.5 and 12 EQs of magnitude between 4 and 4.6 occurred. Before the

strongest of them, an additional noise amplitude reduction of Type I is recorded. After it, two small additional reductions of Type I which can be connected with EQs are visible. They are followed by one long-lasting additional reduction of Type III, during which four more EQs of magnitudes between 4.2 and 4.9 (two on 30 October and two on 31 October) occurred. The connection of these five EQs with the mentioned reduction is not fully possible to harmonize with the expected possible connections based on the explanation of the previous cases and those given in Nina et al. (2020). Namely, increases in  $A_{\text{noise}}$  are expected after each of the first three EQs due to their lower intensity and several hours apart from the next one. However, a large number of weaker earthquakes occurred in this period and their impact on the considered signal should not be excluded *a priori* (the potential connection of weaker earthquakes with  $A_{\text{noise}}$  reductions is reported in Nina et al. (2020)).

- 1–3 November. Before the last three EQs in the observed period,  $A_{\text{noise}}$  is around 2 dB and higher for a certain period of time and, in all three cases, reductions of this parameter is visible (the first reduction is of Type I, and the second two also correspond mostly to this type).

Based on the above analysis, one can conclude that the reduction of  $A_{\text{noise}}$  with the characteristics described in Nina et al. (2020) is recorded in the case of all three earthquakes of magnitudes over 5 (5.5, 6.1 and 6.5) (Cheloni et al., 2017; Galli et al., 2017). The earthquakes of magnitudes from 4 to 5 mostly (25 out of 28 cases) occurred after these 3 higher intensity earthquakes when  $A_{\text{noise}}$  is already reduced. In those cases, the additional observed reduction is either weakened or absent. In three cases when  $A_{\text{noise}}$  is around 2 dB or higher in the period before the change, visible reductions of  $A_{\text{noise}}$  are recorded. A corresponding reduction is also recorded before the magnitude 3.9 earthquake with the epicentre in the CI-2 area during the first analysed day (without stronger earthquakes in the CI-1 area). In other words, the obtained results indicate that the detectability of the noise amplitude reduction is reduced if its value is previously reduced due to the influence of other earlier EQ events. This conclusion opens up an additional question: Are signals with low noise amplitude suitable for analyses of its reduction

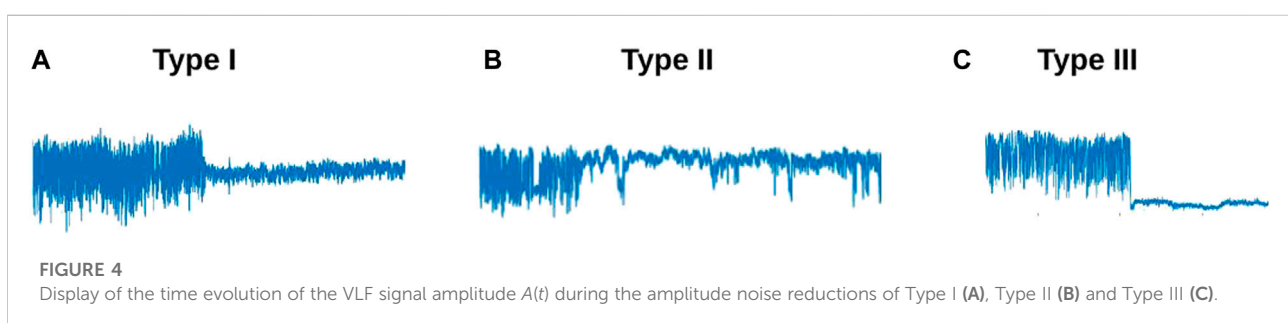
as a potential precursor of earthquakes? In addition, the obtained results indicate the necessity to exclude the temporally close EQs from statistical analyses of effects of various parameters related to the characteristics of the analysed earthquakes, VLF signal and the environment in which it spreads to the noise amplitude reduction properties as such frequent EQs could simultaneously affect the signal.

The analysis of the connection between the  $A_{\text{noise}}$  reductions of the mentioned types and the occurrence of earthquakes whose magnitude is not less than 4 shows that the majority of Type I reductions (8 out of 10, i.e. 80%) and the only recorded Type II reduction are accompanied by observed phenomenon, which is in agreement with the study given in Nina et al. (2020). Although an earthquake was recorded after the Type III reduction on 30 October 2016, the previous analysis and the absence of that connection in the paper Nina et al. (2020) indicate that these phenomena are most likely not related.

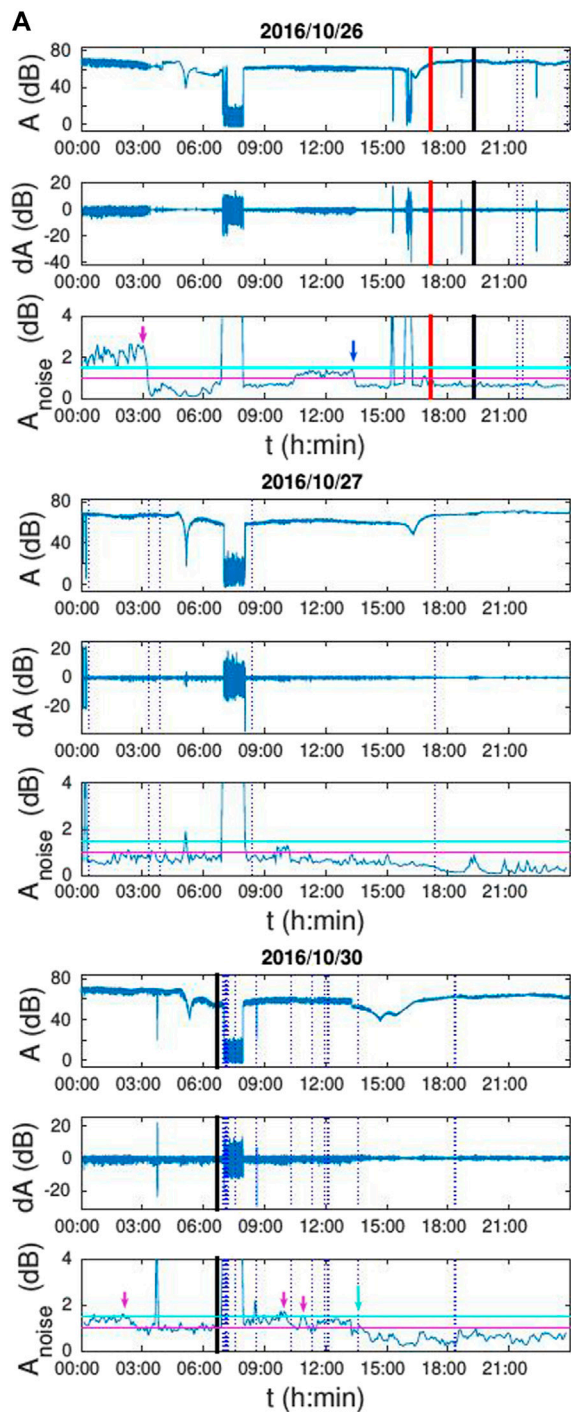
In order to compare the presented analysis for PISA and periods without EQs, we additionally analyse the 6 days before and 6 days after those considered in this study. Based on the corresponding graphs and the detailed analysis given in the Supplementary Material, it can be seen that the reductions of all three types are also visible in these periods. However, out of a total of 18 reductions, 8 (4 of Type I, 3 of Type II and 1 of Type III) are in periods when the intensity of the amplitude is changed (e.g. in ST periods), 3 (all of Type III) are in the period of bad meteorological conditions, 1 (of Type II) in the period when the amplitude is unexpectedly low for the corresponding part of the day, while 4 (1 of Type I and 3 of Type II) have the same value as during most of the day but are preceded by short-term increases in  $A_{\text{noise}}$ . The only two  $A_{\text{noise}}$  reductions that have the properties of those described for PISA and in Nina et al. (2020) are reductions of Type III that, based on the previous analysis, cannot be considered as potential earthquake precursors.

### 3.1.2 The comparison of time evolutions of three VLF signal amplitude characteristics

The analysis presented in the previous section shows that the noise amplitude reductions can be clearly associated with the strongest earthquakes that occurred on 26 and 30 October, as well as the three earthquakes recorded from 1 to 3 November. In



### DHO - Germany



### JXN - Norway

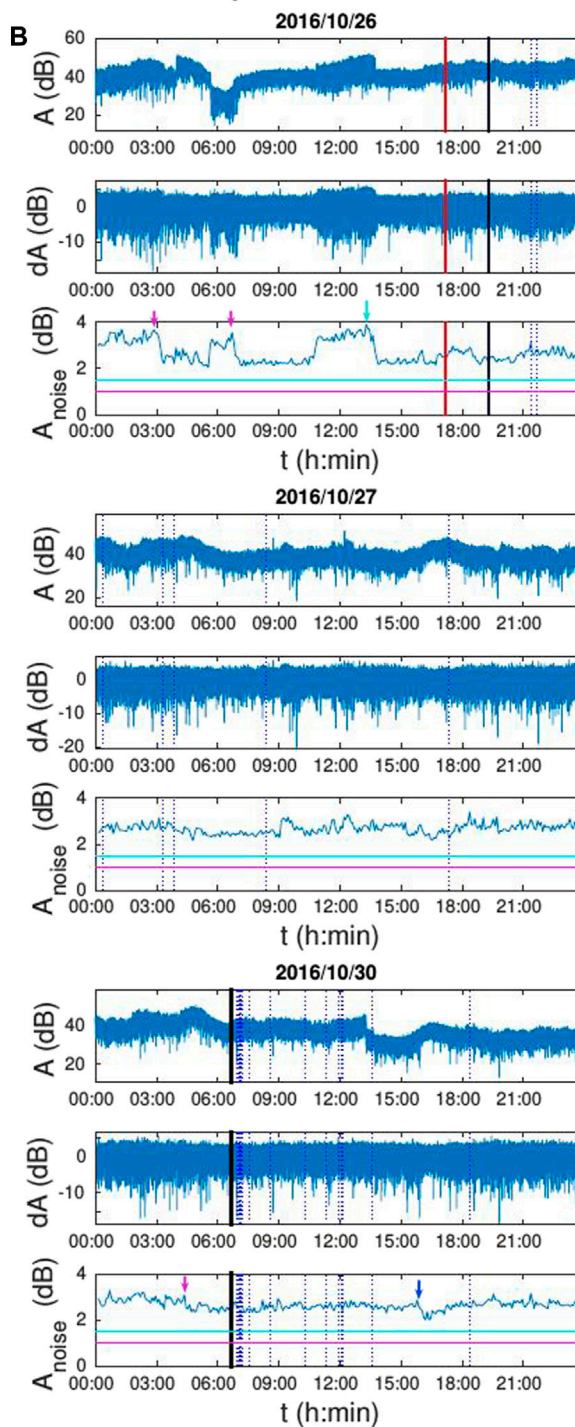
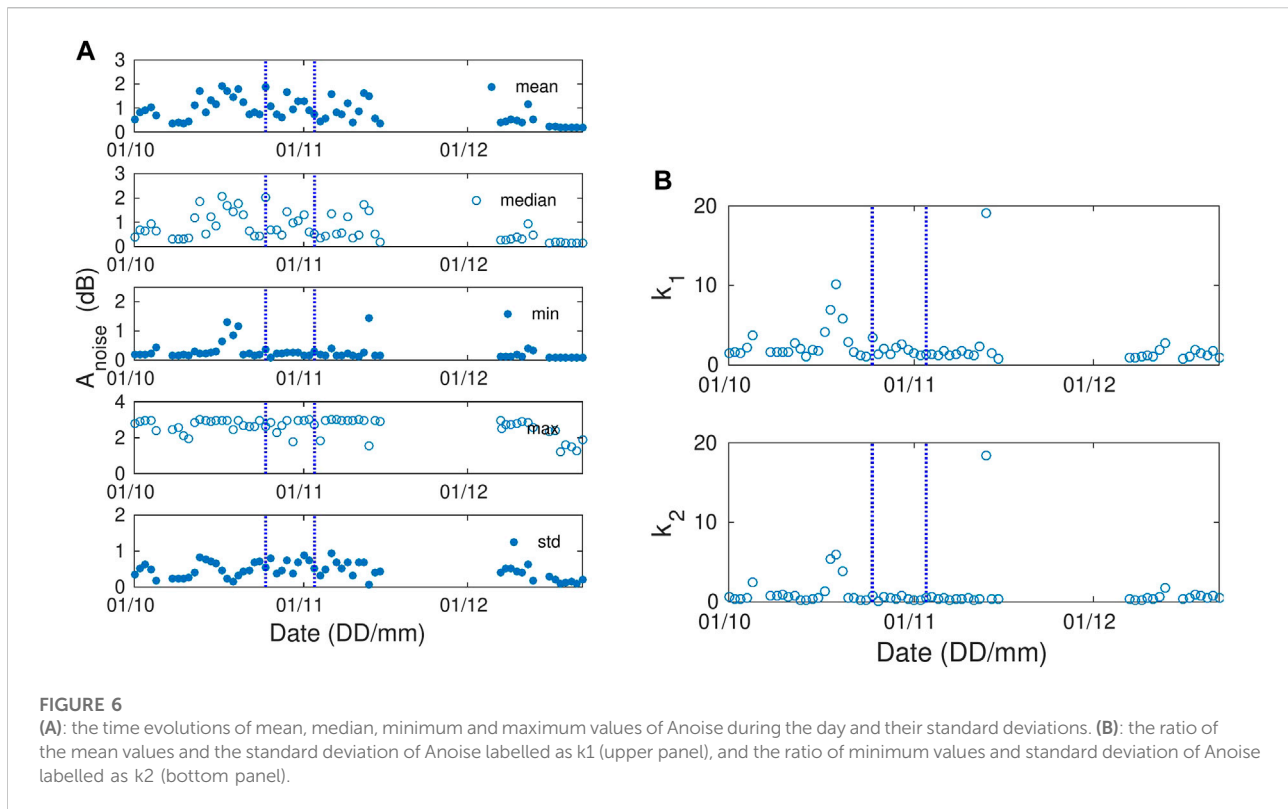


FIGURE 5

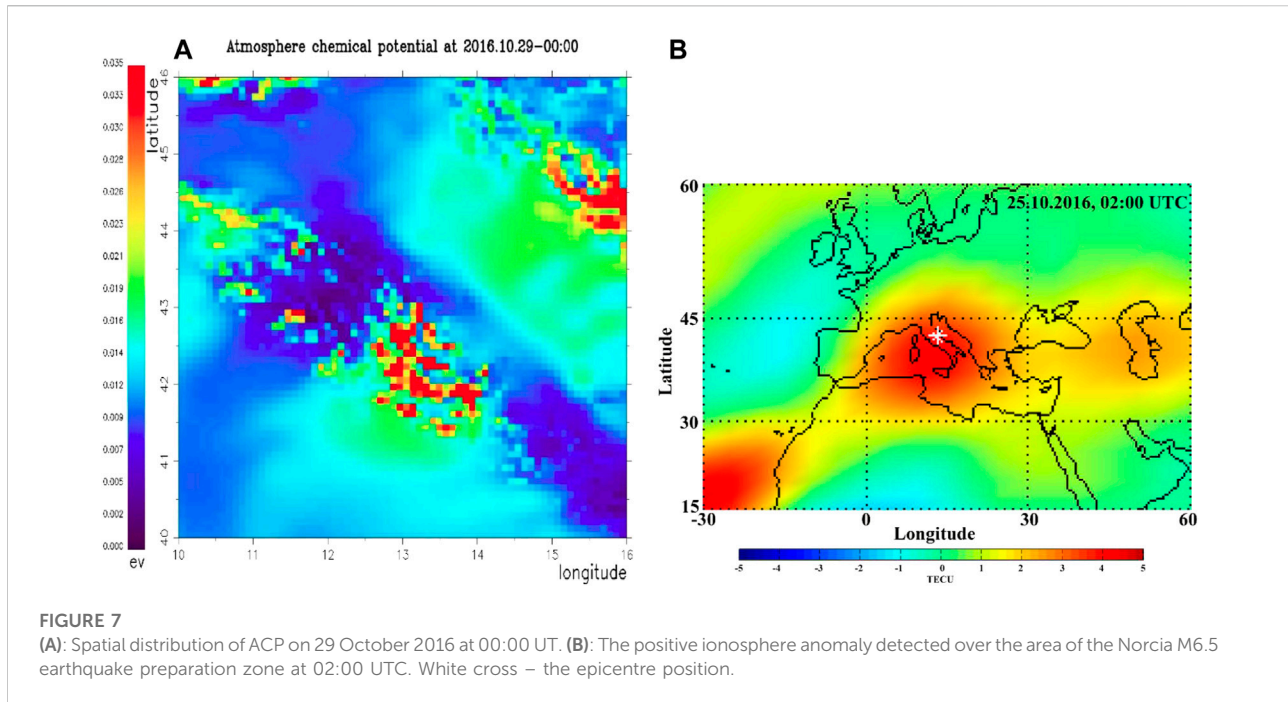
The time evolutions of the recorded amplitude  $A$  (upper panels), its deviation,  $dA$ , from the base curve (middle panels), and the sum amplitude,  $A_{noise}$ , (lower panels) for the DHO (A) and JXN (B) signal on 26 (upper panels), 27 (middle panels) and 30 (bottom panels) October 2016. Vertical lines indicate the times of earthquakes of magnitude  $4 \leq M < 5$  (blue dot lines),  $5 \leq M < 6$  (red line) and  $6 \leq M$  (black lines). Horizontal magenta and cyan lines indicate the amplitude of 1 and 1.5 dB, respectively. The beginnings of the amplitude noise reductions of Type I, II and III are indicated by the magenta, blue and cyan arrows, respectively.



the following analysis we examine localization of the perturbations by processing two additional signal amplitudes in the case of the three strongest EQs, and during 27 October when no earthquake of magnitude greater than 5 was recorded. We consider the DHO and JYN signals that spread in the areas from their transmitters located in Germany and Norway, respectively, to the receiver in Belgrade. As one can see in Figure 1A the ICV signal propagation path is closest to the CI-1 area and it is located south of the seismic active zone. The paths of the other signals pass through areas north of the epicentres of the observed earthquakes.

The time evolutions of these signals for the mentioned 3 days are shown in Figure 5. In the case of the first day, the two noise amplitude reductions (for the ICV signal) associated in the previous Section with the EQs of magnitudes of 5.5 and 6.1 are visible in both reference signals. The  $A_{\text{noise}}$  reductions are almost twice smaller for the farthest signal from the CI-1 area (JXN) than for the ICV signal, while in the case of the DHO signal, the increase in  $A_{\text{noise}}$  between these reductions is significantly smaller than for the ICV signal, which decreases the intensity of the second reduction. In the case of the EQ of the 6.5 magnitude that occurred on 3 November, the  $A_{\text{noise}}$  reductions are similar for all signals, except that the least pronounced is the JYN signal, which, in addition to being the furthest from the seismically active area, also has the largest  $A_{\text{noise}}$  during quiet conditions.

Based on this analysis, we can conclude that the  $A_{\text{noise}}$  reduction is visible in all three signals in the case of the strongest observed earthquakes. This indicates the possibility that the perturbed area has larger dimensions or that it is drifted closer to the receiver (in this way, more observed signals pass through a smaller area). Here it is important to point out that the existence of differences in the changes of  $A_{\text{noise}}$ , as well as the impossibility of establishing connections between their values, and the values of the signal amplitudes (e.g., the time evolutions of  $A_{\text{noise}}$  are similar for the ICV and DHO although the amplitude of the DHO signal is significantly higher than the other two) or  $A_{\text{noise}}$  (e.g., the difference in  $A_{\text{noise}}$  between the two reductions visible on 26 October between the DHO signal, and the ICV signal although their previous  $A_{\text{noise}}$  are very similar) are important for this study. Namely, they indicate that, although they are recorded for several signals, these changes are probably not the result of an unstable reception, but rather reflect variations of atmospheric parameters that can be spatially variable. This conclusion is supported by the difference in the time evolutions of the  $A_{\text{noise}}$  of the JXN signal from those of the other signals (first of all, the absence of the  $A_{\text{noise}}$  reduction at the end of October 27 in the case of the JXN signal, although they are similar for the remaining two signals), as well as the fact that the observed reductions occurred at different parts of the day when the same influence of man-made factors is not expected.



### 3.2 Daily characteristics of the noise amplitude

To examine the long-term variations of the signal amplitude, we analyse the time evolutions of noise amplitude characteristics on a daily basis for the time period from 1 October to 22 December (data for some days are missing due to absence of detection of the ICV signal by the AbsPAL receiver in Belgrade). Figure 6A shows the mean, median, minimum, and maximum noise amplitude values during day, as well as the corresponding standard deviation. The displayed values are obtained after eliminating the data during the period when either the signal was not detected by the AbsPAL receiver in Belgrade, or the noise amplitude is unusually high (indicating periods of solar terminators or the presence of some sudden disturbance). For the shown values, the criterion for this elimination is  $A_{\text{noise}} = 3$  dB (this value is by 1 dB higher than  $A_{\text{noise}}$  in quiet conditions, which makes it possible to eliminate the consideration of perturbations that are a consequence of the mentioned causes which are not related to seismic processes). The essential influence of the choice of this value on the obtained conclusions is excluded by an additional check of the limiting values of 2.5 and 3.5 dB.

The obtained time evolutions of the observed parameters show the following:

- The mean and median values of  $A_{\text{noise}}$  start to increase on October 12 (13 days before PISA). The end point of this

period cannot be exactly determined due to lack of data, but it is evident that from 7 December these values are reduced to those at the beginning of the shown period. In addition to the increases of the considered parameters, the dispersions of the displayed points are also increased in this period. Variations of the standard deviation of the  $A_{\text{noise}}$  values before PISA are more clearly defined, and its saturation is visible in the last considered week (later than the dependence of daily mean and median values of  $A_{\text{noise}}$ ).

- The minimum values of  $A_{\text{noise}}$  are very similar during the entire observed time interval with clearly observed peaks at 5–8 days before and 10 days after PISA, respectively.
- The maximum values of  $A_{\text{noise}}$  are reduced at the beginning and end of the observed time interval as well as during 3 isolated days (1 during PISA and 2 after it).
- The times of the expressed peaks of the mean, median and minima of  $A_{\text{noise}}$  values before and after PISA correspond to the expressed minima of the standard deviation. This can be clearly seen in the form of pronounced maxima in the right panels in Figure 6 that show the time evolutions of the ratio of the mean values and the standard deviation of  $A_{\text{noise}}$ , indicated as  $k_1$  (upper panel), and the ratio of minimum values and standard deviation of  $A_{\text{noise}}$  indicated as  $k_2$  (lower panel).

The above conclusions point to changes in the daily characteristics of  $A_{\text{noise}}$  that begin about 2 weeks before PISA and end no later than about a month after PISA.

### 3.3 Comparisons with other studies

The presented analysis of the noise amplitude in a localized area during PISA is a pioneer study and the confirmation of the obtained conclusions requires additional case studies or statistical research which should be carried out in future. However, a comparison of the study of the VLF signal characteristics related to separated relatively strong EQs given in [Nina et al. \(2020\)](#) and [Nina et al. \(2021a\)](#) indicates similarities with conclusions obtained in this study for the corresponding periods. The potential horizontal displacements and enlargements of the area related to the seismic zone indicated in this study are also shown in the studies of the atmospheric chemical potential (ACP) and TEC. Although they refer to atmospheric areas near the surface and, primarily, in the upper ionosphere, respectively, their comparisons with variations in VLF signals propagating between Earth surface and the lower ionosphere are relevant because the seismo-ionospheric anomalies are not limited by some fixed altitude of the ionosphere but are continued to the upper altitudes into the magnetosphere forming the field-aligned irregularities of electron concentration ([Pulinets et al., 2002](#)). The physical nature of ACP, and the physical interfaces of the lithosphere-ionosphere coupling (generation of ACP) and atmosphere-ionosphere coupling (generation of TEC anomalies) are described in, for example, [Pulinets et al. \(2015a\)](#) and [Pulinets et al. \(2018b\)](#). The common agent of the link between the ACP and TEC are the complex ions formed in the process of the Ion Induced Nucleation (INN). The sharp (hyperbolic) growth of large complex ions concentration and their hydration leads to the growth of ACP. Simultaneously the same complex ions sharply decrease the conductivity of the atmospheric column between the ground and ionosphere increasing the ionospheric potential (IP) and forming the positive anomalies of TEC. The physical mechanism of the seismo-ionospheric coupling and statistical proofs of connection of an earthquake with TEC variations is described in [Pulinets and Boyarchuk \(2004\)](#); [Pulinets et al. \(2015b\)](#); [Pulinets et al. \(2018\)](#); [Liu et al. \(2018\)](#). In addition, the observed diurnal changes exhibit some characteristics similar to those identified in many studies describing different types of ionospheric disturbances. In the following text, we point out these similarities and agreements.

#### 3.3.1 The noise amplitude reductions

As stated in [Section 3.1.1](#), the  $A_{\text{noise}}$  reductions connected with the EQs that occurred during the period when the noise amplitude corresponds to that in quiet conditions have characteristics very similar to those shown in [Nina et al. \(2021b\)](#) for all EQs of magnitudes  $M \geq 4$  as well as for 9 EQs of magnitudes  $M \leq 4$ .

Contrary to the results presented in [Nina et al. \(2021b\)](#) where the noise amplitude reductions are visible only for the ICV signal, the analysis performed in this study shows corresponding changes for several VLF signals. As stated in [Section 3.1.2](#),

this may be due to a larger area influenced by seismic activity or its drifting towards the location of the receiver. Both mentioned phenomena have already been presented in the literature ([Biagi et al., 2012](#)). The study presented in [Sanchez-Dulcet et al. \(2015\)](#) indicates a combination of both possibilities as well as the temporal variability of the spatial distribution of atmospheric disturbances. The larger perturbed area through which the considered VLF signals propagate is also consistent with the spatial distribution of ACP around the time of the Norcia M6.5 earthquake that occurred on 30 October 2016 (see [Figure 7A](#)). This parameter is the so-called integrated parameter actually been the proxy of the radon activity and its measurement at the 100 m altitude can be used for estimation of the disturbed area ([Pulinets et al., 2015](#)). The considered anomaly activity shown in this map covers (and exceeds) the whole region of Italian seismic activity during 2009–2017 presented in [Soldati et al. \(2020\)](#) ([Soldati et al., 2020](#)). Finally, the spatial distribution of TEC, presented in [Figure 7B](#), shows a large disturbed area which includes the region around the receiver location.

#### 3.3.2 Daily characteristics of the noise amplitude

As stated in Introduction, studies in the literature primarily point to ionospheric variations that start a few days or several hours before major earthquakes. These variations apply to both the low and high ionosphere. Variations detected by VLF/LF signals occur in the form of the amplitude minimum time shift during solar terminator periods (the so-called “terminator time”) ([Hayakawa, 1996](#); [Molchanov et al., 1998](#); [Yamauchi et al., 2007](#); [Yoshida et al., 2008](#); [Maurya et al., 2016](#)), signal amplitude variations ([Biagi et al., 2001a,b](#); [Zhao et al., 2020](#)), and periodic fluctuations ([Miyaki et al., 2001](#); [Molchanov et al., 2001](#); [Rozhnoi et al., 2004](#); [Biagi et al., 2006](#); [Hayakawa et al., 2010](#); [Ohya et al., 2018](#)). These variations can be detected using different methods such as analyses of the standard deviation, the Wavelet spectra, the terminator time, deviations from mean values, and the Principal Component Analysis ([Hayakawa, 1996](#); [Biagi et al., 2012](#)). Analyses of the GNSS signals indicate variation in TEC a few days before the considered EQ events. Examples of these changes can be seen in, for example, [Pulinets and Davidenko \(2018a\)](#) and [Abdennasser and Abdelmansour \(2019\)](#). In addition, it is found that the pre-seismic anomalies related to the acoustic-gravity waves, energetic particle burst in radiation belt, magnetic field, electron density, electron temperature and surface latent heat flux are recorded several days before EQs (see, for example, [Sasmal et al. \(2021\)](#); [Chowdhury et al. \(2022\)](#); [Ghosh et al. \(2022\)](#)).

The results obtained in this study are in agreement with those reported in the literature. Namely, as stated in [Section 3.1.2](#), the beginnings of changes in the time evolution of the analysed parameters that describe the noise amplitude are visible about 2 weeks (increases in mean and median values of  $A_{\text{noise}}$  and dispersion of relevant points in plots of the corresponding time evolutions), a week (peaks of minimum values of  $A_{\text{noise}}$  and values

of parameters  $k_1$  and  $k_2$ ), and on the day of the beginning of PISA (increasing the dispersion of the standard deviation  $A_{\text{noise}}$ ).

Based on the comparison mentioned in Sections 3.3.1, 3.3.2, we can conclude that the presented analysis shows a confirmation of the previously presented variations of VLF signals, which are stated as possible precursors of earthquakes.

## 4 Conclusion

In this paper, we presented an analysis of VLF signal noise amplitude variations during the period of intense seismic activity in Central Italy from 25 October to 3 November 2016. It is a continuation of the study of possible connection between the noise amplitude reduction and earthquakes that can be analysed independently of other relevant connections due to a sufficiently large time interval between earthquake events and, in some cases, large spatial distances between their epicentres. In this study we analysed additional particular earthquake events and extended the global research to examination of a possible influence of the intense seismic activity to the observed signal characteristic changes. That was possible because we observed a time period when almost 1000 earthquakes (31 of them had a magnitude of 4 or greater, and the maximum magnitudes were 5.5, 6.1 and 6.5) were registered in a small area in Central Italy within only 10 days.

In this study we processed the amplitudes of the ICV, DHO and JXN signals emitted in Italy, Germany, the USA and Norway, respectively, and recorded in Belgrade, Serbia. The main analysis is performed for the ICV signal amplitude, while examination of other signal amplitude characteristics was done in order to analyse the localization of changes and possible variations in the noise amplitude due to problems in signal reception.

We presented analyses of: (1) the noise amplitude reduction which were first pointed out as potential precursors of earthquakes in the case of the Kraljevo earthquake that occurred in Serbia on 3 November 2010; (2) the daily characteristics of the VLF signal noise amplitude in the period from 1 October to 22 December, performed for the first time in this study.

Based on the results of the presented research, we can conclude the following facts:

- A significant reduction in the noise amplitude that can be associated with one or more earthquakes affects the possibility of detecting isolated significant reductions that can be associated with a particular earthquake.
- The noise amplitude reduction is recorded for all three earthquakes of magnitudes greater than 5, which is in agreement with the results shown for the earthquakes near Kraljevo, and the Tyrrhenian and Western Mediterranean Sea (presented in the first study that examines the considered correlations). It is important to emphasize that two of these three earthquakes occurred within about 2 h and can be related to the same reduction of the noise amplitude.
- Earthquakes of magnitudes between 4 and 5 that do not follow more intense earthquakes can also be connected with clear specific reductions in the noise amplitude, unlike those after more intense earthquakes for which additional reductions of already low noise amplitudes are small or completely absent.
- There are three types of the noise amplitude reduction depending on whether the noise amplitude reduction is a consequence of the increasing lower and/or decreasing higher amplitude values. Based on the analyses shown in this study and in Nina et al. (2020), correlations between these reductions and earthquakes can be established in cases of the increasing lower and decreasing higher amplitude values (Type I), or when the increase of the lower amplitude values is recorded (Type II). In the cases of decreasing higher amplitude values (Type III), an appropriate correlation with the occurrence of earthquakes was not established.

These conclusions indicate the importance of the noise amplitude value in quiet conditions for the detection of its reduction which can be potentially connected with an earthquake. In other words, the application of low noise amplitude signals for the detection of potential precursors of these natural disasters is questioned. In addition, this study opens more questions that require statistical studies. They relate to the possibility of more the noise amplitude reduction before a strong earthquake or more (relatively) strong earthquakes, increase the unperturbed area through which the VLF signals propagate during the long-term intensification of seismic activity (i.e. a large number of earthquakes in a relatively short period), displacement of the area under influence of the seismic activity relative to the seismically active area, and existence of changes in daily noise amplitude characteristics several days before the intensification of seismic activity (an increase in the noise amplitude mean and median values, clearly defined oscillations of its standard deviation followed by an increase in the dispersion of points in the graph of its time evolution at the beginning of the period of the earthquake series, the short-term (1 day to a few days) peaks of the ratio of the mean/minimum noise amplitude values and its standard deviation before and after the period of intense seismic activity, and the increase of its minimum values). Analyses of these issues should be the focus of future studies. In addition, due to the complexity of the analyzed connection caused by the possibility of the influence of a large number of parameters describing the earthquake, the VLF signal and the environment in which it spreads, it is necessary to carry out a larger number of studies in order to (if possible) define the criteria (in different conditions) for establishing a connection between the noise amplitude reductions and earthquake occurrences.

Here, we point out that analyses of the VLF signal characteristics are not sufficient to obtain the necessary information about localization (vertical and horizontal) of perturbed area. For this reason, it is necessary to do more

studies based on different kinds of observation data so that theoretical analyses and models can be provided. This issue will be subject of future investigation, too.

At the end, we emphasize that the results of this, the second, study of examining the possibility that the noise amplitude reduction of VLF signals is a precursor of earthquakes contribute to the statistic that indicates that such a conclusion is quite realistic. Namely, as in the case of the first relevant study where the observed type of connection was recorded for all recorded earthquakes with magnitude greater than 4 and with epicentres close to the observed signal path (4 events), this analysis also shows that such a connection is detectable in all cases when there is no influence of other events (all 6 events including two events close in time which are connected with the same reduction). This confirmation gives even more importance to the continuation of the relevant research.

## Data availability statement

Requests for the VLF data used for analysis can be directed to the corresponding author. The other datasets used for this study can be found in <http://www.emsc-csem.org/Earthquake/>, <https://eswd.eu/cgi-bin/eswd.cgi>, [https://www-app3.gfz-potsdam.de/kp\\_index/Kp\\_ap\\_Ap\\_SN\\_F107\\_since\\_1932.txt](https://www-app3.gfz-potsdam.de/kp_index/Kp_ap_Ap_SN_F107_since_1932.txt), [https://hesperia.gsfc.nasa.gov/goes/goes\\_event\\_listings/](https://hesperia.gsfc.nasa.gov/goes/goes_event_listings/).

## Author contributions

Conceptualization, methodology, investigation, resources, formal analysis, writing—original draft, preparation, visualization, AN; Software, data curation, AN, SM, VČ, and MU; Validation, PB, SP, LP, GN, and MR; Writing—review and editing, all authors. All authors have read and agreed to the published version of the manuscript.

## Funding

The authors acknowledge funding provided by the Institute of Physics Belgrade, the Astronomical Observatory (the contract

## References

- Abdenasser, T., and Abdelmansour, N. (2019). Geodetic contribution to predict the seismological activity of the Italian metropolis by the ionospheric variant of GPS\_TEC. *J. Atmos. Solar-Terrestrial Phys.* 183, 1–10. doi:10.1016/j.jastp.2018.12.006
- Ammar, A., and Ghalila, H. (2016). Ranking of sudden ionospheric disturbances by means of the duration of VLF perturbed signal in agreement with satellite X-ray flux classification. *Acta Geophys.* 64, 2794–2809. doi:10.1515/acgeo-2016-0114
- Basak, T., and Chakrabarti, S. K. (2013). Effective recombination coefficient and solar zenith angle effects on low-latitude D-region ionosphere evaluated from vlf

signal amplitude and its time delay during X-ray solar flares. *Astrophys. Space Sci.* 348, 315–326. doi:10.1007/s10509-013-1597-9

Biagi, P., Castellana, L., Maggipinto, T., Piccolo, R., Minafra, A., Ermini, A., et al. (2006). Lf radio anomalies revealed in Italy by the wavelet analysis: Possible preseismic effects during 1997–1998. *Phys. Chem. Earth, Parts A/B/C* 31, 403–408. doi:10.1016/j.pce.2005.10.001

Biagi, P. F., Maggipinto, T., Righetti, F., Loiacono, D., Schiavulli, L., Ligonzo, T., et al. (2011). The European VLF/LF radio network to search for earthquake precursors: Setting up and natural/man-made disturbances. *Nat. Hazards Earth Syst. Sci.* 11, 333–341. doi:10.5194/nhess-11-333-2011

## Acknowledgments

The Kilpisjarvi VLF data were supplied by the Sodankyla Geophysical Observatory, University of Oulu, Finland. For checking of the meteorological conditions we used information given on the European Severe Weather Database website. For checking of the geomagnetic conditions we used information provided by the Geomagnetic Observatory Niemegk, GFZ German Research Centre for Geosciences.

## Conflict of interest

Author SM was employed by the company Novelic.

The remaining authors declare that the research was conducted in the absence of any commercial or financial relationships that could be construed as a potential conflict of interest.

## Publisher's note

All claims expressed in this article are solely those of the authors and do not necessarily represent those of their affiliated organizations, or those of the publisher, the editors and the reviewers. Any product that may be evaluated in this article, or claim that may be made by its manufacturer, is not guaranteed or endorsed by the publisher.

## Supplementary material

The Supplementary Material for this article can be found online at: <https://www.frontiersin.org/articles/10.3389/fenvs.2022.1005575/full#supplementary-material>



- Biagi, P. F., Piccolo, R., Ermini, A., Martellucci, S., Bellecci, C., Hayakawa, M., et al. (2001a). Disturbances in LF radio-signals as seismic precursors. *Ann. Geophys.* 44, 4. doi:10.4401/ag-3552
- Biagi, P. F., Piccolo, R., Ermini, A., Martellucci, S., Bellecci, C., Hayakawa, M., et al. (2001b). Possible earthquake precursors revealed by LF radio signals. *Nat. Hazards Earth Syst. Sci.* 1, 99–104. doi:10.5194/nhess-1-99-2001
- Biagi, P., Righetti, F., Maggipinto, T., Schiavulli, L., Ligonzo, T., Ermini, A., et al. (2012). Anomalies observed in VLF and LF radio signals on the occasion of the Western Turkey earthquake (Mw= 5.7). *Int. J. Geosciences* 19, 2011. doi:10.4236/ijg.2012.324086
- Calais, E., and Minster, J. (1998). GPS, earthquakes, the ionosphere, and the space shuttle. *Phys. Earth Planet. Interiors* 105, 167–181. doi:10.1016/S0031-9201(97)00089-7
- Chakrabarti, S. K., Sasmal, S., and Chakrabarti, S. (2010). Ionospheric anomaly due to seismic activities – part 2: Evidence from D-layer preparation and disappearance times. *Nat. Hazards Earth Syst. Sci.* 10, 1751–1757. doi:10.5194/nhess-10-1751-2010
- Chakraborty, S., and Basak, T. (2020). Numerical analysis of electron density and response time delay during solar flares in mid-latitude lower ionosphere. *Astrophys. Space Sci.* 365, 184–189. doi:10.1007/s10509-020-03903-5
- Cheloni, D., De Novellis, V., Albano, M., Antonioli, A., Anzidei, M., Atzori, S., et al. (2017). Geodetic model of the 2016 central Italy earthquake sequence inferred from InSAR and GPS data. *Geophys. Res. Lett.* 44, 6778–6787. doi:10.1002/2017GL073580
- Chowdhury, S., Kundu, S., Ghosh, S., Hayakawa, M., Schekotov, A., Potirakis, S. M., et al. (2022). Direct and indirect evidence of pre-seismic electromagnetic emissions associated with two large earthquakes in Japan. *Nat. Hazards (Dordr.)* 112, 2403–2432. doi:10.1007/s11069-022-05271-5
- Davies, K., and Baker, D. M. (1965). Ionospheric effects observed around the time of the Alaskan earthquake of March 28, 1964. *J. Geophys. Res.* 70, 2251–2253. doi:10.1029/JZ070i009p02251
- Fu, C.-C., Wang, P.-K., Lee, L.-C., Lin, C.-H., Chang, W.-Y., Giuliani, G., et al. (2015). Temporal variation of gamma rays as a possible precursor of earthquake in the longitudinal valley of eastern Taiwan. *J. Asian Earth Sci.* 114, 362–372. doi:10.1016/j.jseaes.2015.04.035
- Galli, P., Castenetto, S., and Peronace, E. (2017). The macroseismic intensity distribution of the 30 October 2016 earthquake in central Italy ( $M_w$ 6.6): Seismotectonic implications. *Tectonics* 36, 2179–2191. doi:10.1002/2017TC004583
- Ghosh, S., Chowdhury, S., Kundu, S., Sasmal, S., Politis, D. Z., Potirakis, S. M., et al. (2022). Unusual surface latent heat flux variations and their critical dynamics revealed before strong earthquakes. *Entropy* 24 (1), 23. doi:10.3390/e24010023
- Grubor, D. P., Šulić, D. M., and Žigman, V. (2008). Classification of X-ray solar flares regarding their effects on the lower ionosphere electron density profile. *Ann. Geophys.* 26, 1731–1740. doi:10.5194/angeo-26-1731-2008
- Hayakawa, M., Horie, T., Muto, F., Kasahara, Y., Ohta, K., Liu, J.-Y., et al. (2010). Subionospheric VLF/LF probing of ionospheric perturbations associated with earthquakes: A possibility of earthquake prediction. *SICE J. Control, Meas. Syst. Integration* 3, 10–14. doi:10.9746/jcmsi.3.10
- Hayakawa, M. (1996). The precursory signature effect of the kobe earthquake on VLF subionospheric signals. *J. Comm. Res. Lab.* 43, 169–180. doi:10.1109/ELMAGC.1997.617080
- He, L., Wu, L., Heki, K., and Guo, C. (2022). The conjugated ionospheric anomalies preceding the 2011 Tohoku-Oki earthquake. *Front. Earth Sci. (Lausanne)* 10, 23. doi:10.3389/feart.2022.850078
- Hegai, V., Kim, V., and Liu, J. (2006). The ionospheric effect of atmospheric gravity waves excited prior to strong earthquake. *Adv. Space Res.* 37, 653–659. doi:10.1016/j.asr.2004.12.049
- Inan, U. S., Lehtinen, N. G., Moore, R. C., Hurley, K., Boggs, S., Smith, D. M., et al. (2007). Massive disturbance of the daytime lower ionosphere by the giant  $\gamma$ -ray flare from magnetar SGR 1806-20. *Geophys. Res. Lett.* 34, L08103. doi:10.1029/2006GL029145
- Kolarski, A., Grubor, D., and Šulić, D. (2011). Diagnostics of the solar X-flare impact on lower ionosphere through seasons based on VLF-NAA signal recordings. *Balt. Astron.* 20, 591–595.
- Korepanov, V., Hayakawa, M., Yampolski, Y., and Lizunov, G. (2009). AGW as a seismo-ionospheric coupling responsible agent. *Phys. Chem. Earth, Parts A/B/C* 34, 485–495. doi:10.1016/j.pce.2008.07.014
- Leonard, R. S., Barnes, J., and Barnes, R. A. (1965). Observation of ionospheric disturbances following the Alaska earthquake. *J. Geophys. Res.* 70, 1250–1253. doi:10.1029/JZ070i005p01250
- Liperovsky, V. A., Pokhotelov, O. A., Meister, C. V., and Liperovskaya, E. V. (2008). Physical models of coupling in the lithosphere-atmosphere-ionosphere system before earthquakes. *Geomagn. Aeron.* 48, 795–806. doi:10.1134/S0016793208060133
- Liu, J.-Y., Hattori, K., and Chen, Y.-I. (2018). Application of total electron content derived from the global navigation satellite system for detecting earthquake precursors. *Am. Geophys. Union (AGU)* 17, 305. doi:10.1002/9781119156949.ch17
- Maekawa, S., Horie, T., Yamauchi, T., Sawaya, T., Ishikawa, M., Hayakawa, M., et al. (2006). A statistical study on the effect of earthquakes on the ionosphere, based on the subionospheric LF propagation data in Japan. *Ann. Geophys.* 24, 2219–2225. doi:10.5194/angeo-24-2219-2006
- Matzka, J., Stolle, C., Yamazaki, Y., Bronkalla, O., and Morschhauser, A. (2021). The geomagnetic kp index and derived indices of geomagnetic activity. *Space weather.* 19, e2020SW002641. doi:10.1029/2020SW002641
- Maurya, A. K., Venkatesham, K., Tiwari, P., Vijaykumar, K., Singh, R., Singh, A. K., et al. (2016). The 25 April 2015 Nepal earthquake: Investigation of precursor in vlf subionospheric signal. *J. Geophys. Res. Space Phys.* 121, 416. doi:10.1002/2016JA022721
- Mitra, A. P. (Editor) (1974). *Ionospheric effects of solar flares* (Dordrecht: Astrophysics and Space Science Library), 46.
- Miyaki, K., Hayakawa, M., and Molchanov, O. (2001). “The role of gravity waves in the lithosphere - ionosphere coupling, as revealed from the subionospheric LF propagation data,” in *Seismo electromagnetics: Lithosphere - atmosphere - ionosphere coupling* (Tokyo: TERRAPUB), 229–232.
- Molchanov, O., Hayakawa, M., and Miyaki, K. (2001). VLF/LF sounding of the lower ionosphere to study the role of atmospheric oscillations in the lithosphere-ionosphere coupling. *Adv. Polar Up. Atmos. Res.* 15, 146–158.
- Molchanov, O., Hayakawa, M., Oudoh, T., and Kawai, E. (1998). Precursory effects in the subionospheric vlf signals for the kobe earthquake. *Phys. Earth Planet. Interiors* 105, 239–248. doi:10.1016/S0031-9201(97)00095-2
- Molina, C., Boudriki Semlali, B.-E., Park, H., and Camps, A. (2022). A preliminary study on ionospheric scintillation anomalies detected using gnss-r data from NASA CYGNSS mission as possible earthquake precursors. *Remote Sens.* 14, 2555. doi:10.3390/rs14112555
- Némec, F., Santolík, O., and Parrot, M. (2009). Decrease of intensity of ELF/VLF waves observed in the upper ionosphere close to earthquakes: A statistical study. *J. Geophys. Res.* 114, 4. doi:10.1029/2008JA013972
- Nina, A., Biagi, P. F., Mitrović, S. T., Pulinet, S., Nico, G., Radovanović, M., et al. (2021a). Reduction of the VLF signal phase noise before earthquakes. *Atmosphere* 12, 444. doi:10.3390/atmos12040444
- Nina, A., Nico, G., Mitrović, S. T., Čadež, V. M., Milošević, I. R., Radovanović, M., et al. (2021b). Quiet ionospheric D-region (qiondr) model based on VLF/LF observations. *Remote Sens.* 13, 483. doi:10.3390/rs13030483
- Nina, A., Pulinet, S., Biagi, P., Nico, G., Mitrović, S., Radovanović, M., et al. (2020). Variation in natural short-period ionospheric noise, and acoustic and gravity waves revealed by the amplitude analysis of a VLF radio signal on the occasion of the Kraljevo earthquake (mw = 5.4). *Sci. Total Environ.* 710, 136406. doi:10.1016/j.scitotenv.2019.136406
- Nina, A., Simić, S., Srećković, V. A., and Popović, L. Č. (2015). Detection of short-term response of the low ionosphere on gamma ray bursts. *Geophys. Res. Lett.* 42, 8250–8261. doi:10.1002/2015GL065726
- Ohya, H., Tsuchiya, F., Takishita, Y., Shinagawa, H., Nozaki, K., and Shiokawa, K. (2018). Periodic oscillations in the d region ionosphere after the 2011 tohoku earthquake using LF standard radio waves. *J. Geophys. Res. Space Phys.* 123, 5261–5270. doi:10.1029/2018JA025289
- Oyama, K. I., Devi, M., Ryu, K., Chen, C. H., Liu, J. Y., Liu, H., et al. (2016). Modifications of the ionosphere prior to large earthquakes: Report from the ionosphere precursor study group. *Geosci. Lett.* 3, 6. doi:10.1186/s40562-016-0038-3
- Perrone, L., De Santis, A., Abbattista, C., Alfonsi, L., Amoroso, L., Carbone, M., et al. (2018). Ionospheric anomalies detected by ionosonde and possibly related to crustal earthquakes in Greece. *Ann. Geophys.* 36, 361–371. doi:10.5194/angeo-36-361-2018
- Pulinet, S. A., and Davidenko, D. V. (2018a). The nocturnal positive ionospheric anomaly of electron density as a short-term earthquake precursor and the possible physical mechanism of its formation. *Geomagn. Aeron.* 58, 559–570. doi:10.1134/s0016793218040126
- Pulinet, S. A., Ouzounov, D. P., Karelin, A. V., and Davidenko, D. V. (2015a). Physical bases of the generation of short-term earthquake precursors: A complex model of ionization-induced geophysical processes in the lithosphere-atmosphere-ionosphere-magnetosphere system. *Geomagn. Aeron.* 55, 521–538. doi:10.1134/S0016793215040131
- Pulinet, S. A., Ouzounov, D. P., Karelin, A. V., and Davidenko, D. V. (2015b). Physical bases of the generation of short-term earthquake precursors: A complex

model of ionization-induced geophysical processes in the lithosphere-atmosphere-ionosphere-magnetosphere system. *Geomagn. Aeron.* 55, 521–538. doi:10.1134/S0016793215040131

Pulinets, S., Boyarchuk, K., Hegai, V., and Karelin, A. (2002). *Conception and model of seismo-ionosphere-magnetosphere coupling*. Tokyo: TERRAPUB, 353–361.

Pulinets, S., and Boyarchuk, K. (2004). *Ionospheric precursor of earthquakes*. Heidelberg, Germany: Springer.

Pulinets, S., Ouzounov, D., Karelin, A., and Boyarchuk, K. (2022). *Earthquake precursors in the atmosphere and ionosphere: New concepts*. Berlin, Heidelberg, Germany: Springer.

Pulinets, S., Ouzounov, D., Karelin, A., and Davidenko, D. (2018b). *Lithosphere-atmosphere-ionosphere-magnetosphere coupling—a concept for pre-earthquake signals generation*. America: American Geophysical Union AGU. 77–98. doi:10.1002/9781119156949.ch6

Pulinets, S., and Ouzounov, D. (2011). Lithosphere-atmosphere-ionosphere coupling (LAIC) model – An unified concept for earthquake precursors validation. *J. Asian Earth Sci.* 41, 371–382. doi:10.1016/j.jseas.2010.03.005

Rozhnoi, A., Solovieva, M., Molchanov, O., and Hayakawa, M. (2004). Middle latitude lf (40 khz) phase variations associated with earthquakes for quiet and disturbed geomagnetic conditions. *Phys. Chem. Earth, Parts A/B/C* 29, 589–598. doi:10.1016/j.pce.2003.08.061

Sanchez-Dulcet, F., Rodríguez-Bouza, M., Silva, H. G., Herraiz, M., Bezzeghoud, M., and Biagi, P. F. (2015). Analysis of observations backing up the existence of VLF and ionospheric TEC anomalies before the Mw6.1 earthquake in Greece, January 26, 2014. *Phys. Chem. Earth Parts A/B/C* 85, 150–166. doi:10.1016/j.pce.2015.07.002

Sasmal, S., and Chakrabarti, S. K. (2009). Ionospheric anomaly due to seismic activities; part 1: Calibration of the VLF signal of VTX 18.2 kHz station from Kolkata and deviation during seismic events. *Nat. Hazards Earth Syst. Sci.* 9, 1403–1408. doi:10.5194/nhess-9-1403-2009

Sasmal, S., Chowdhury, S., Kundu, S., Politis, D. Z., Potirakis, S. M., Balasis, G., et al. (2021). Pre-seismic irregularities during the 2020 Samos (Greece) earthquake (M = 6.9) as investigated from multi-parameter approach by ground and space-based techniques. *Atmosphere* 12 (8), 1059. doi:10.3390/atmos12081059

Schmitter, E. D. (2013). Modeling solar flare induced lower ionosphere changes using VLF/LF transmitter amplitude and phase observations at a midlatitude site. *Ann. Geophys.* 31, 765–773. doi:10.5194/angeo-31-765-2013

Soldati, G., Cannelli, V., and Piersanti, A. (2020). Monitoring soil radon during the 2016–2017 central Italy sequence in light of seismicity. *Sci. Rep.* 10, 13137. doi:10.1038/s41598-020-69821-2

Sorokin, V., and Yashchenko, A. (1999). Disturbances of conductivity and electric field in the earth-ionosphere layer over an earthquake preparation focus. *Geomagnetism Aeronomy* 39, 228–234. doi:10.1023/A:1021549612290

Thomson, N. R., Rodger, C. J., and Clilverd, M. A. (2005). Large solar flares and their ionospheric D region enhancements. *J. Geophys. Res.* 110, A06306. doi:10.1029/2005JA011008

Wang, J., Huang, Q., Ma, Q., Chang, S., He, J., Wang, H., et al. (2020). Classification of VLF/LF lightning signals using sensors and deep learning methods. *Sensors* 20, 1030. doi:10.3390/s20041030

Xiong, P., Long, C., Zhou, H., Battiston, R., De Santis, A., Ouzounov, D., et al. (2021). Pre-earthquake ionospheric perturbation identification using cses data via transfer learning. *Front. Environ. Sci.* 9, 4. doi:10.3389/fenvs.2021.779255

Yamauchi, T., Maekawa, S., Horie, T., Hayakawa, M., and Soloviev, O. (2007). Subionospheric VLF/LF monitoring of ionospheric perturbations for the 2004 mid-niigata earthquake and their structure and dynamics. *J. Atmos. Solar-Terrestrial Phys.* 69, 793–802. doi:10.1016/j.jastp.2007.02.002

Yoshida, M., Yamauchi, T., Horie, T., and Hayakawa, M. (2008). On the generation mechanism of terminator times in subionospheric VLF/LF propagation and its possible application to seismogenic effects. *Nat. Hazards Earth Syst. Sci.* 8, 129–134. doi:10.5194/nhess-8-129-2008

Yuen, P. C., Weaver, P. F., Suzuki, R. K., and Furumoto, A. S. (1969). Continuous, traveling coupling between seismic waves and the ionosphere evident in May 1968 Japan earthquake data. *J. Geophys. Res.* 74, 2256–2264. doi:10.1029/JA074i009p02256

Zhao, S., Shen, X., Liao, L., Zhima, Z., Zhou, C., Wang, Z., et al. (2020). Investigation of precursors in VLF subionospheric signals related to strong earthquakes (M > 7) in western China and possible explanations 7) in western China and possible explanations. *Remote Sens.* 12, 3563. doi:10.3390/rs12213563

Žigman, V., Grubor, D., and Šulić, D. (2007). D-region electron density evaluated from VLF amplitude time delay during X-ray solar flares. *J. Atmos. Solar-Terrestrial Phys.* 69, 775–792. doi:10.1016/j.jastp.2007.01.012